Thermal Curing Behavior of MWCNT Modified Vinyl Ester-Polyester Resin Suspensions Prepared with 3-Roll Milling Technique

A. T. SEYHAN,[1] ALEJANDRA DE LA VEGA,[2] M. TANOGLU,[3] K. SCHULTE[2]

[1]Department of Materials Science and Engineering, Anadolu University, Iki Eylul Campus, 26550 Eskisehir, Turkey

[2]Institute of Polymers and Polymer Composites, Technical University Hamburg-Harburg (TUHH), Denickestrasse 15, D-21073 Hamburg, Germany

[3]Department of Mechanical Engineering, İzmir Institute of Technology (IZTECH) 35437, İzmir, Turkey

ABSTRACT: This study aims to investigate the curing behavior of a vinyl ester-polyester resin suspensions containing 0.3 wt % of multiwalled carbon nanotubes with and without amine functional groups (MWCNTs and MWCNT-NH$_2$). For this purpose, various analytical techniques, including Differential Scanning Calorimetry (DSC), Fourier infrared spectroscopy (FTIR), Raman Spectroscopy, and Thermo Gravimetric Analyzer (TGA) were conducted. The resin suspensions with carbon nanotubes (CNTs) were prepared via 3-roll milling technique. DSC measurements showed that resin suspensions containing CNTs exhibited higher heat of cure (Q), besides lower activation energy (E_a) when compared with neat resin. For the sake of simplicity of interpretation, FTIR investigations were performed on neat vinyl ester resin suspensions containing the same amount of CNTs as resin. As a result, the individual fractional conversion rates of styrene and vinyl ester were interestingly found to be altered dependent on MWCNTs and MWCNT-NH$_2$. The findings obtained from RS measurements of the cured samples are highly proportional to those obtained from FTIR measurements. TGA measurements revealed that CNT modified nanocomposites have higher activation energy of degradation (E_d) compared with the cured polymer. The findings obtained revealed that CNTs with and without amine functional groups alter overall thermal curing response of the surrounding matrix resin, which may probably impart distinctive characteristics to mechanical behavior of the corresponding nanocomposites achieved. © 2009 Wiley Periodicals, Inc. J Polym Sci Part B: Polym Phys 47: 1511–1522, 2009

Keywords: differential scanning calorimeter (DSC); FTIR; multiwalled carbon nanotubes; radical polymerization; Raman spectroscopy; thermal gravimetric analysis (TGA)

INTRODUCTION

Incorporation of nanosized fillers into polymer matrices is this study of interest to manufacture functional nanocomposites with superior properties. Carbon nanotubes (CNTs) with high aspect

ratio coupled with low density and huge specific surface area (SSA) exhibit exceptional mechanical, thermal, and electrical properties, which make them excellent filler candidates for polymeric materials.[1–4] However, they demonstrate strong tendency to form dense agglomerates within polymers, which affects adversely the ultimate performance of their resultant nanocomposites. Therefore, interfacial bonding and proper dispersion of individual CNTs within the surrounding polymers are the keys to improving final properties of polymers.[5–8] In general, some chemical functional groups are grafted onto the surfaces of CNTs to promote their compatibility with the surrounding matrix resin.[4–8] In particular, commercial methods used for dispersion of CNTs in thermosetting polymers such as epoxy include sonication and high speed mechanical stirring. Alternatively, Gojny et al.[1] employed 3-roll milling to prepare CNT modified epoxy resin suspensions. They concluded that dispersion of CNTs via 3-roll milling is better than that of CNTs via sonication or mechanical stirring.

Unsaturated polyester (UP) and vinyl ester (VE) resins are the most common matrix materials utilized for reinforced composite structures. VE resins possess some superior properties including chemical resistance, low viscosity, relatively high mechanical properties, as well as low cost and ability to cure at room temperature.[6–10] At a given weight content, CNTs with high aspect ratio and surface area are expected to affect the curing reaction of the corresponding polymer matrices in a more significant manner compared with carbon black (CB) microparticles.[3–7]

In general, cure kinetic modeling expressions may be phenomenological or mechanistic. The phenomenological models are related to the main features and do not take into account every chemical reaction which occurs in the system of interest.[8–11] They are based on the assumption that the exothermic heat evolved during the cure reaction is proportional to the extent of monomer conversion in the system. If the cure reaction is very complicated, the phenomological models are commonly preferred for the cure kinetic calculations.[8] Isothermal DSC measurements differ from the nonisothermal ones in that they have complete separation between the variables of time and temperature. However, a significant development of the cure state can occur before DSC reaches and stabilizes at the desired temperature. As a result, the reaction may not reach the completion at lower temperatures. Alternatively, dynamic DSC measurements could provide a better capture of

the cure kinetics at both the on-set and the end of the reaction.[10–14] However, DSC measures in principle only the overall heat release during the reaction, but can not distinguish multiple overlapping reactions that occur within the resin system. The main emphasis with DSC is on gathering data to develop empirical models like the autocatalytic kinetic model, which are system specific and thus not representative for all styrene/VE or UP systems.[15–21] At this stage, researches focused further their attention on Fourier infrared spectroscopy (FTIR) spectrometry, which offers the potential to differentiate the rate of isothermal reactions dependent on the spectral changes of different functional groups.[8–10] FTIR allows depletion of the reactive species in a sample to be monitored in a separate manner, provided that their absorption peaks are noticeable from the product peaks of interest.

Raman spectrometry (RS) is a simple nondestructive technique. Like FTIR spectrometry, it can provide a spectrum of characteristic bandwidths that help identify the chemical species and bond types present in the material of interest.[22] One advantage of the Raman technique over FTIR is that any shift in characteristic Raman peaks can be attributed to straining of the material, through external and internal stressing.[9] In this respect, Raman spectrometry has recently been used to identify CNTs, evaluate their dispersion in polymers, and highlight the interaction between polymer matrix and CNTs.[17] In this technique, interaction of CNTs with polymers is reflected by a peak shift or a peak width change.

Understanding of thermal stability of polymer composites is of significance to interpret the effect of filler constituents embedded in polymer matrices on the chemical degradation mechanism of the final product. Thermogravimetric analysis (TGA) is one of the most commonly used thermal analysis techniques to monitor the thermal decomposition of polymeric materials. In principle, thermoanalytical curves, for instance DSC curves, provide only basic information about the process and do not make fine distinction between partial chemical reactions during thermal degradation process.

In summary, the combination of experimental techniques mentioned above helps assess any chemical interaction between reinforcement constituent and the surrounding polymer matrix in the best way possible.

In our earlier study,[18] it was found that addition of multiwalled carbon nanotubes with and

without amine functional groups (MWCNTs and MWCNT-NH$_2$) in VE-polyester resin blend altered considerably the rheological and thermomechanical properties of the resulting suspensions and their nanocomposites, respectively. In this study, the cure behavior of the same resin system containing 0.3 wt % of MWCNTs and MWCNT-NH$_2$ was reported in detail. 3-Roll milling that applies high shear forces on the resin suspensions was used for proper dispersion of the CNTs within styrene free polyester resin. The collected dispersion was then blended with VE resin via mechanical stirrer to achieve final resin suspensions. Analytical techniques including Differential scanning calorimeter (DSC), FTIR, RS, and TGA were then employed to explore the effect of MWCNTs and MWCNT-NH$_2$ on radical assisted polymerization of the polymer matrix, with particular emphasis on amine functional groups over the surfaces of CNTs.

EXPERIMENTAL

Materials

MWCNTs and MWCNT-NH$_2$ were obtained from Nanocyl (Namur Belgium) and used as additives for the resin system involved. They have the same average diameter of 15 nm. However, MWCNTs have a length of approximately 50 μm, while MWCNT-NH$_2$ have a length of $\sim$10 μm, which is five times less than that of MWCNTs. POLIYA 420 styrene-free isophtalic acid-based polyester resin, and POLIVEL 701 VE resin, which is a mixture based on 65 wt % of bisphenol A-based dimethacrylate VE prepolymer and 35 wt % of styrene comonomer, were provided by POLIYA Polyester, Turkey. The formulized resin blend was composed of 25 wt % of POLIYA 420 and 75 wt % of POLİVES 701. Paraffin based styrene emission agent (BKY 740 from Alton Chemie, Germany) was used to prevent evaporation of styrene from the resin blend during polymerization. BKY 740 was further added to the resin system at a ratio of 1 wt % of the resin blend prepared. Cobalt naphtanate (CoNAP), a solution containing 6 wt % of active cobalt, and methyl ethyl kethone peroxide (MEKP) were used, respectively, as accelerator and initiator to polymerize the resin suspensions.

3-Roll Milling Process

To prepare the resin suspensions, 0.3 wt % of MWCNTs and MWCNT-NH$_2$ were dispersed within styrene free resin Poliya 420 by shear intensive blending, using the 3-roll milling method. The collected CNT/polyester resin suspension was then blended with VE resin by hand and mechanical stirring for about 10 and 30 min, respectively. To avoid reagglomeration of CNTs during mixing, blending process was performed in a cooled water bath. After addition of BKY 740 to the blend, the CoNAP and MEKP were introduced to the system at a ratio of 0.2 and 1 wt %, respectively. Please note that CNTs were placed into a vacuum oven at 80 °C for half an hour prior to processing to preclude possible water adsorption from the atmosphere onto surface of CNTs. In subsequence, the catalyzed suspensions were immediately subjected to nonisothermal DSC scanning to eliminate any experimental error due to sudden initiation of polymerization reaction. Please note that a special resin mixture was employed to avoid the difficulties with 3-roll milling. Instant evaporation of styrene due to heat evolved gave rise to the viscosity of the resin suspensions left on the rolls. Further, the resin left on the rolls become too sticky and jelly due to ongoing styrene evaporation during 3-roll milling. This makes it impossible to provide the required accuracy for reproducibility of the resin dispersions at the same quality due to unknown content of styrene left in the final resin dispersion obtained. To overcome this problem, a specially synthesized styrene free polyester resin was utilized, which has a viscosity high enough to apply intensive shear in between the rolls, thus enhancing the dispersion state of CNTs within the polyester resin. Indeed, based on the rheological measurements performed earlier, the optimal viscosity was found to be around 800 cP for the resin to be processed with 3-roll milling in an efficient manner.

DSC Measurements

All measurements were performed by a Shimadzu DSC-50 scanning calorimeter. A small quantity of the sample (10–25 mg) was used for the DSC studies in a sealed aluminium pan. Dynamic runs were carried out on the suspensions, using another aluminium empty cell as a reference. The curing thermal data for each sample was obtained from dynamic scans at different heating rates (5, 10, and 20 °C/min) from room temperature up to 200 °C in a nitrogen atmosphere. The measurements for each sample were repeated three times. The total heat of the reaction was estimated for

each sample from the nonisothermal experiments by integrating the area under peaks of the DSC exotherms obtained.

Cure Kinetic Approach via DSC

The basic kinetic approach of thermosetting polymers is that the heat flow measured in DSC is proportional to both overall heat release and the rate of the kinetic process, as given below.[8,9]

$$\frac{d\alpha}{dt} = \frac{\phi}{Q} \tag{1}$$

where Q is the enthalpy of the curing reaction and ϕ is the measured heat flow, (α) is the extent of the reaction. For the nonisothermal conditions, α is obtained by integrating the eq 1[14] by utilization of constant heating rate

$$\alpha = \frac{1}{Q \cdot \beta} \int_{T_i}^{T} \phi \cdot dT \tag{2}$$

where β is the heating rate ($\beta = dT/dt$) and T_i refers to the beginning of the baseline approximation. The rate of kinetic process can be expressed as a function of temperature dependent rate constant. The rate constant $K(T)$ and (α) dependent kinetic model function $f(\alpha)$ is as follows.[7–9,14]

$$\frac{d\alpha}{dt} = K(T) \cdot f(\alpha) \tag{3}$$

$K(T)$ in eq 3 follows Arrhenius form, as given in eq 4.[5]

$$K(T) = A \cdot \exp\left(-\frac{E_a}{RT}\right) \tag{4}$$

Where A is the pre-exponential factor, E_a is the apparent activation energy, R is the gas constant and T is the absolute temperature. In the case of nonisothermal conditions with constant heating rate $\beta = dT/dt$, eq 3 and 4 can be combined and revised into the form, as given below[5,9]

$$\frac{d\alpha}{dT} = \frac{A}{\beta} \cdot \exp\left(-\frac{E_a}{RT}\right) \cdot f(\alpha) \tag{5}$$

E_a values are determined from the plot of $1/T_i$ versus $\ln(\beta_i/T_i^2)$ as a function of degree of cure.[5] T_i is the temperature within the DSC exotherm area at which the value of enthalpy is taken. The value of enthalpy is related to the degree of cure achieved at T_i.

FTIR Measurements

Cure monitoring of VE resin containing 0.3 wt % of MWCNTs and MWCNT-NH$_2$ were performed by utilizing Schimadzu FTIR spectrometer in transmission mode. Please note that only neat VE resin was used as matrix material to ease the interpretation of data because, in the case of a complex mixture of polymers, it would be hard to differentiate which bands come from which molecules.[16–19] As VE resin contains styrene, CNTs were blended with VE resin via mechanical stirring to avoid evaporation of styrene. The FTIR spectra of MWCNTs and MWCNT-NH$_2$ were also taken to correlate the data obtained for their corresponding nanocomposites. The point herein is to just reflect the impact of individual CNTs or their agglomerates on the free radical polymerization. In this manner, the same measured quantity of CoNAP and MEKP as in the production of the nanocomposites was added to neat liquid VE resin and its CNT modified suspensions to initiate the polymerization reaction. A drop of this catalyzed mixture was then taken and compressed between two potassium bromide (KBr) transparent crystal plates. This plate of sample was placed into a sealed infrared liquid cell which allows the curing process to be monitored in real time while preventing instant evaporation of styrene. The samples prepared were eventually scanned from 500 to 4000 cm^{-1} at a resolution of 4 cm^{-1}.

Cure Kinetics Approach via FTIR

FTIR spectroscopy was used to monitor the depletion of carbon–carbon double bonds (C=C) for styrene and VE systems in separate manner. In this respect, the absorbance at 945 cm^{-1} and 910 cm^{-1} were monitored during curing to determine the conversion of both of the monomers. Note that the peaks at 945 cm^{-1} and 910 cm^{-1} correspond to out of plane bending of carbon–hydrogen bonds in the vinyl group of the VE monomer and wagging of CH$_2$ in the vinyl group of the styrene monomer, respectively.[19,20] Aromatic carbon–hydrogen bonds at 830 cm^{-1} in VE and 700 cm^{-1} in styrene were used to correct for the thickness changes in the sample during reaction. Eqs 6 and 7 were then employed to compute normalized fractional conversion of VE and styrene double bonds, respectively.

$$\alpha_{VE}(t) = 1 - \left(\frac{A_t(945\,\text{cm}^{-1})}{A_0(945\,\text{cm}^{-1})}\right) \tag{6}$$

$$\alpha_{ST}(t) = 1 - \left(\frac{A_t(910\,\text{cm}^{-1})}{A_0(910\,\text{cm}^{-1})}\right) \quad (7)$$

In the equation, α is the fractional conversions of double bonds associated with each corresponding monomer at time t, and A_0 and A_t are the normalized absorbance peaks before the reaction starts and after a certain time t. The magnitudes of the relevant absorbance peaks were measured, considering slight shifts in peak locations and base lines due to reaction. In this respect, automatic sampling was performed at specified time intervals and the measurements were terminated once no changes were observed in the absorbance peak area. Please note that, to ease the data interpretation, base line corrected FTIR spectra of MWCNTs and MWCNT-NH$_2$ were subtracted from the base line corrected spectra of the nanocomposites prior to calculation of the area under the corresponding peaks.

Raman Spectroscopy (RS) Measurements

Raman spectrometry were performed on CNTs, the cured polymer and its nanocomposites prepared with MWCNTs and MWCNT-NH$_2$, using Renishaw 2000 Ramanscope, equipped with He–Ne laser, 50 cm^{-1} notch filter, and a 600 groove per mm grating. The wave length and power of laser were set to 633 nm and 20 mW, respectively. The spectra collection time was set to 60 s to achieve a low noise to signal ratio. The spectra were acquired from 100 to 3500 cm^{-1} to detect especially the D and G bands of the CNTs. For the sake of accurate interpretation similar to that in FTIR, the effect of MWCNTs and MWCNT-NH$_2$ on the depletion of C=C of neat resin was evaluated by subtracting the spectrum of the resultant nanocomposites from the spectrum of each corresponding CNTs. The consequent spectrum and the obtained spectrum of the cured neat polymer were mutually compared for evaluation. In this respect, the corresponding peak areas were considered.

Thermal Gravimetric Analyzer (TGA) Measurements

A Perkin–Elmer Pyris 1 TGA was used for investigation of thermal degradation response of the cured polymer and its resultant nanocomposites containing 0.3 wt % of MWCNTs and MWCNT-NH$_2$. A sample of about 10 mg for each batch was placed into alumina crucible. The samples were

then heated from ambient temperature up to 700 °C in a 50 mL/min nitrogen flow at different heating rates (5, 10, and 20 °C/min). Eventually, sample temperature, sample weight and its first derivative were recorded as a function of time.

Kinetic Approach to Thermal Decomposition

Flynn and Wall[23] proved that at a constant degree of conversion, C, the activation energy of thermal degradation, E_d for a reaction is related to the heating rate, β, and the temperature, T, by the following Arrhenius equation;

$$E_d = -(R/b)\frac{\Delta(\log\beta)}{\Delta(1/T)} \quad (8)$$

where b is a constant with a value of 0.475 K^{-1}. The value of E_d can be determined from a plot of logarithm of heating rate versus the reciprocal of the absolute temperature at constant conversion level such that the slope of $\log\beta$ versus $1/T$ equals to E_d. Note that E_d values considered in this study was calculated based upon 5 wt % of conversion.

RESULTS AND DISCUSSION

Interactions of Matrix Resin with CNTs

Interactions of CNTs with the surrounding matrix resin are highly critical to ultimate properties of the resulting nanocomposites. Figure 1 is the illustration of chemical interaction between the amino functionalized CNTs and VE resin. As seen in the figure, C—N covalent bonding is supposed to occur between the surfaces of amino functionalized carbon nanotubes and the opened carbon double bonds of VE resin as an example. In addition, weak hydrogen bonds are also supposed to occur as a result of interaction between the hydrogen molecules in VE and those coming from chemical structure of amine groups over the surfaces of CNTs. Please note that the chemical mechanism illustrated in the figure is hypothetical and does not necessarily take place within the resin structure. In fact, there are many critical factors associated with the complex reactions that occur in the resin system. As CNTs exhibit huge surface area and aspect ratio, their interactions with the free radicals generated by the decomposition of the initiator is vastly critical to the characteristics of the network structure formed in the resultant system.
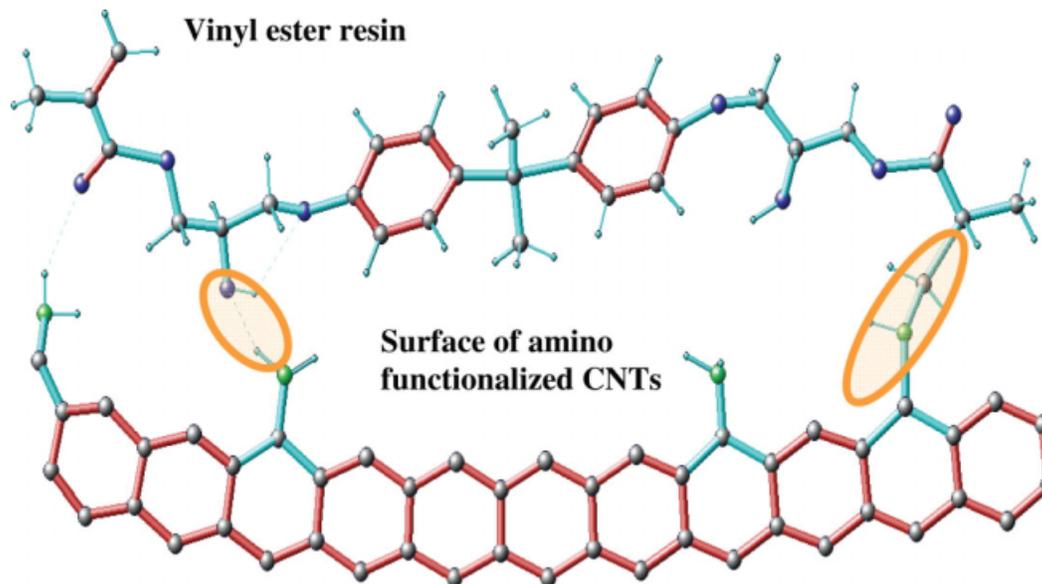
Figure 1. Illustration of chemical interaction between the amino functionalized CNTs and vinyl ester resin.

In our case, amine groups on the surfaces of CNTs react with the either opened double carbon bonds of polyester or VE that are indeed supposed to react with the styrene monomers to form crosslinking. In other words, there may be a competition between styrene and amine groups to react with the double bonds of the matrix resin. As a consequence, the residual styrene monomers would be most probably polymerized as polystyrene without crosslinking the polyester molecules. This may affect the crosslinking density, just tuning the individual fractional conversion of the monomers in the resin system, thus imparting different features to ultimate performance of the resulting nanocomposites. In fact, these interactions are the motivations behind the assembly of this article.
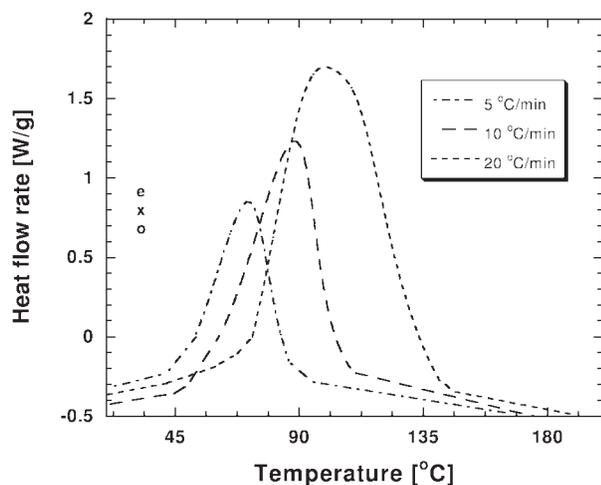
Figures 2–4 show the nonisothermal DSC exotherms obtained at various constant heating rates (5, 10 and 20 °C/min) for the neat resin blend and its suspensions containing MWCNTs and MWCNT-NH$_2$, respectively. By considering the initial (T_i), the peak (T_p), and the final (T_f)
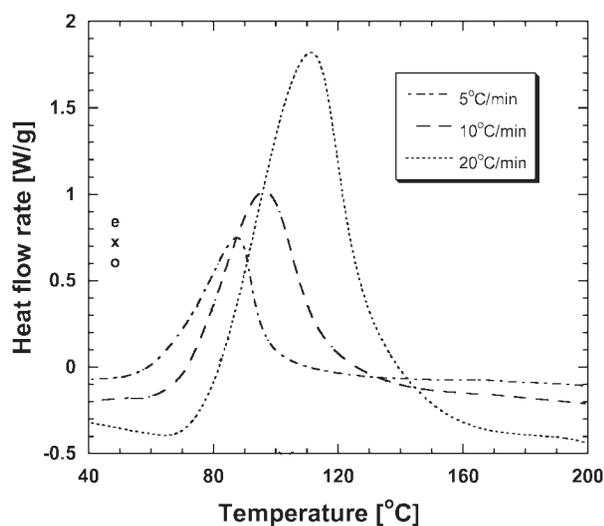
Figure 2. Nonisothermal DSC exotherm at different heating rates for the neat vinyl ester/polyester resin blend.
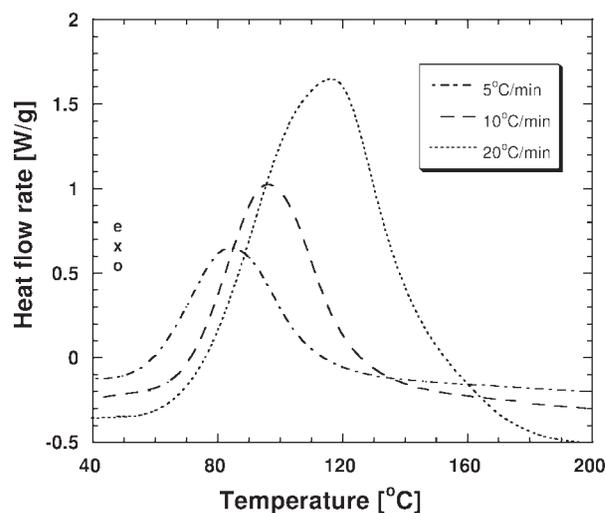
Figure 3. Nonisothermal DSC exotherm at different heating rates for CNT/vinyl ester polyester suspensions containing 0.3 wt % of MWCNT.

Figure 4. Nonisothermal DSC exotherm at different heating rates for CNT/polymer suspensions containing 0.3 wt % of MWCNT-NH$_2$

temperatures, and by calculating the reaction enthalpy (Q) values from each corresponding DSC exotherm, the impact of CNTs on the cure kinetics of the entire resin system was evaluated. The data obtained was given in Table 1. As seen in the table, incorporation of CNTs into the polymer blend increases the reaction enthalpy at each given heating rate. The resin suspensions with MWCNTs and MWCNT-NH$_2$ exhibited 3 and 10% higher enthalpy values than the neat resin, respectively. Furthermore, T_i value of MWCNT-NH$_2$ modified resin suspensions interestingly appeared to scatter around the same value (40 °C) regardless of the heating rate. This can be considered as ample evidence that amine functional groups grafted onto surfaces of CNTs modify the interfacial interactions between CNTs and the surrounding matrix resin.

Figure 5 gives the variation of E_a for the neat resin blend and CNT-modified suspensions with respect to the degree of cure. Note that E_a values were calculated at 0.05 increments of α values. The results obtained showed that activation energy of each suspension varies with the degree of cure. Even at the room temperature, the curing of thermosetting resins such as VE is highly exothermic. This exothermic reaction gives remarkable rise to the resin temperature, which may lead to the curing reaction to be accelerated in such a way that thermal decomposition of the unanalyzed initiators or even the self-initiation of the monomers may occur during curing.[5,9] Moreover, it was also found that resin blend with carbon nanotubes featured moderately lower E_a values as compared to neat resin blend at each stage of cure. This trend is more obvious for the suspensions with MWCNT-NH$_2$. The E_a values decrease at lower degree of cure but then gradually rise up towards to the end of the curing reaction (α = 1). These predictions show the consistency with our main approach that CNTs alter somewhat the chemical interactions within resin media during curing dependent on the functional groups grafted onto their surfaces. Puglia et al.[3] found that, with increasing MWCNTs contents in an epoxy system, the initial reaction rates increased, while the time to the maximum cure rate decreased. The authors ascribed this compromise to the acceleration effect of MWCNTs. Xie et al.[2] found the similar results on the behavior of CNTs in another epoxy resin system. Moreover, Bae et al.[4] revealed that surface functional groups over the surfaces of CNTs lowered the corresponding activation energy while at the same time reducing the heat of cure, significantly. However, polymerization reaction mechanism of epoxy is different from that of VE. In our case, primary amine groups over the CNTs are likely to react with the double carbon bonds of the resin blend and inhibit free radical reaction to

Table 1. Calorimetric Data Obtained from DSC Experiments Performed on Neat Polymer and CNT/Polymer Suspensions

| Sample	Heating Rate (°C/min)	T_i (°C)	T_p (°C)	T_f (°C)	Q (J/gr)
Neat resin blend	5	59 ± 14	88 ± 9	112 ± 14	216 ± 19
	10	71 ± 12	96 ± 14	127 ± 11	238 ± 29
	20	82 ± 15	110 ± 8	142 ± 13	287 ± 26
Resin blend MWCNTs	5	58 ± 13	86 ± 12	115 ± 18	228 ± 17
	10	69 ± 11	95 ± 17	125 ± 12	242 ± 15
	20	76 ± 18	114 ± 9	152 ± 22	296 ± 11
Resin blend MWCNT-NH$_2$	5	39 ± 5	70 ± 13	92 ± 27	234 ± 22
	10	40 ± 6	90 ± 15	111 ± 24	247 ± 24
	20	41 ± 8	108 ± 18	148 ± 19	312 ± 28
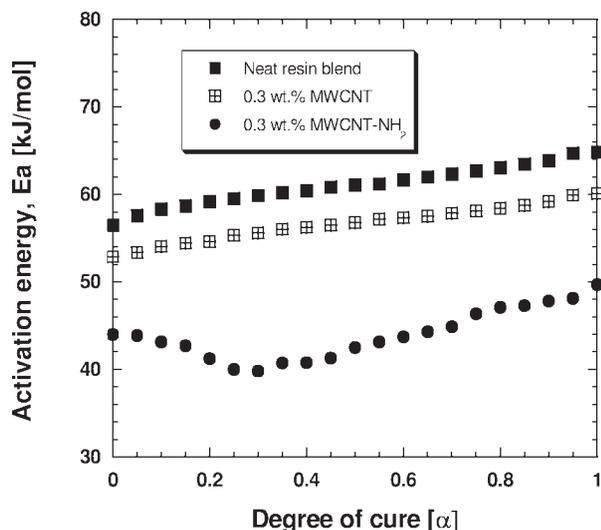
Figure 5. The apparent activation energy (Ea) of the samples with and without any filler as a function of degree of conversion.

some extent, thus reducing the crosslinking density of the resulting cured polymer. On the other hand, amine groups are grafted onto the surfaces of CNTs by ball milling, during which the lengths of the CNTs are partially diminished. In brief, the length of MWCNT-NH$_2$ is five times less than that of MWCNTs. In another respect, relatively low aspect ratio of MWCNT-NH$_2$ due to functionalization process may play a major role in resin cure reactions. Gryschuk et al.[21] stated that aspect ratio and surface area of CNTs are critical to final properties of polymers, and that lower aspect ratio of MWCNTs is more beneficial to ultimate properties of highly crosslinked resins like VE. Moreover, they also concluded that the amount of MEKP and CoNAP subjected to the entire resin system needs to be optimized dependent upon the type of CNTs.

Although thermal analysis by DSC in both isothermal and dynamic modes is widely used to study the kinetics of cure reactions, DSC does not give information about the individual conversion profiles of VE and styrene. However, in our case, the presence of CNTs in the resin system that polymerize via decomposition of radicals could change the relative conversion rates of VE, polyester and styrene double bonds, which produces significant differences in the resulting network structure. In fact, whether the promising results obtained from DSC measurements come mainly from amine functional groups over the surfaces of CNTs or from the reduced aspect ratio of CNTs

via ball milling is still open to discussion. Therefore, it is reasonable to further investigate the interaction of untreated and amino functionalized CNTs with the matrix resin, utilizing more sophisticated analytical tools such as FTIR and RS.

As previously elucidated in details, neat VE resin was utilized as matrix material for FTIR studies to avoid complexity with chemistry of polymer blends. The aim herein is to just reveal the impact of the presence of CNTs with and without amine functional groups on the chain growth polymerization. Figure 6 shows the transmission spectra for a neat VE styrene resin and its suspensions containing 0.3 wt % of MWCNTs and MWCNT-NH$_2$ before and after cure at room temperature (25 °C). As seen in the figure, CNTs with and without amine functional groups have substantial effects on the peak intensity values of neat VE resin. Figure 7, 8, and 9 give experimental plot of fractional double bond conversion of VE and styrene with respect to the reaction time in VE resin and its suspensions with MWCNTs and MWCNT-NH$_2$, respectively, at room temperature (25 °C). These graphs were obtained from the equations described earlier. Please note that double bond conversions of VE and styrene are based on the initial number of double bonds of VE and styrene, respectively. In this respect, a higher value of conversion obtained for VE bonds does not necessarily mean that more number of VE double bonds would react when compared with styrene double bonds. As given in Figure 7, in the very beginning of the reaction, the rate of
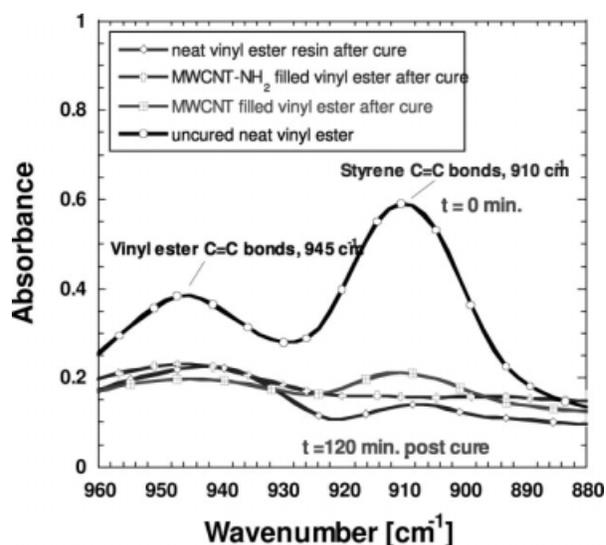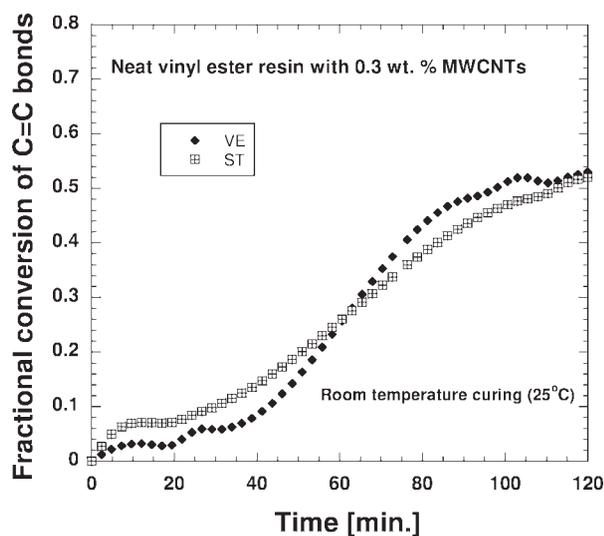

Figure 6. FTIR spectra for neat vinyl ester resin before and after cure.
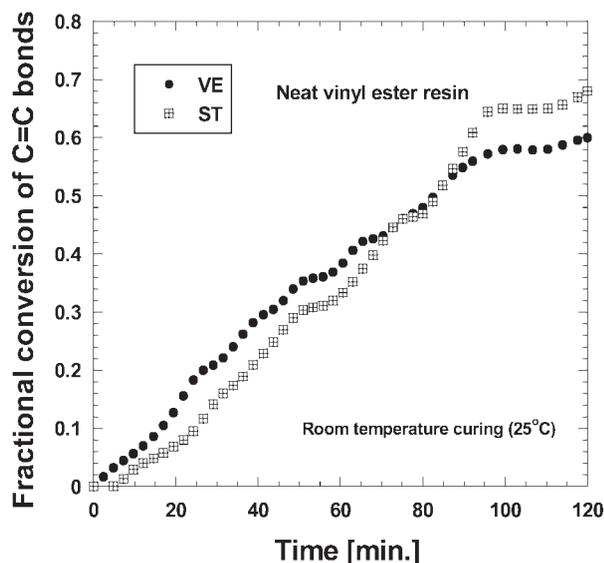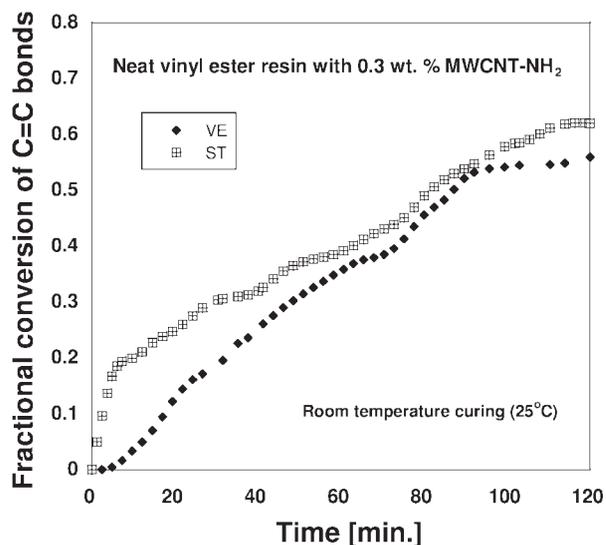
Figure 7. Fractional double bond conversions of vinyl ester and styrene in neat vinyl ester resin as a function of time.

Figure 9. Fractional double bond conversions of vinyl ester and styrene in vinyl ester resin with 0.3 wt % of MWCNT-NH$_2$ as a function of time.

fractional conversion of VE is more than that of styrene. Almost at the end of the reaction, the rate of conversion of styrene exceeded conversion rate of VE. These findings are very consistent with those in other similar studies reported in the literature.[19,20] However, as depicted in Figures 8 and 9, it was observed that the individual fractional conversion rates of styrene and VE were altered dependent on the amine functional groups over the surfaces of CNTs. The final conversion of styrene exceeded the final conversion of VE dou-

ble bonds in the resin suspensions with MWCNT-NH$_2$. Nevertheless, final conversion of VE double bonds is slightly higher than that of styrene in the resin suspensions containing MWCNTs. In this respect, one can conclude that some of amine groups over the surfaces of CNTs react with the double bonds of VE resin during curing which are indeed supposed to react with styrene. In this scenario, residual styrene monomers would be polymerized as polystyrene without crosslinking the VE molecules, as elucidated in the beginning of the discussion section in details. Moreover, regardless of amine functional groups, conversions of styrene and VE double bonds were found to be lower in the CNT modified resin suspensions than in neat VE resin.

In fact, one major parameter associated with curing characteristics of VE resin is vitrification. Vitrification takes place when the T_g exceeds the cure temperature. Once the resin is vitrified, the motions of polymer are remarkably restricted and the reaction is ceased due to diffusion limitations on the growing radical species and on the monomers.[17] Vitrification occurs about 92 min (after which no considerable change in the conversion values are observed) into the cure for the neat VE resin system studied. At this value, the conversion values of 0.56 and 0.64 were obtained for VE and styrene monomers, respectively. However, addition of MWCNTs to VE resin shifts the time at which vitrification occurs to higher values (about 110 and 115 min, respectively), while
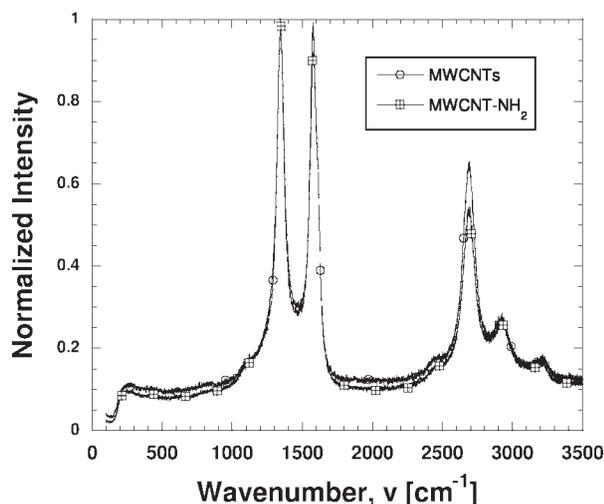

Figure 8. Fractional double bond conversions of vinyl ester and styrene in vinyl ester resin with 0.3 wt % of MWCNTs as a function of time.

Figure 10. Raman spectra of CNTs.[22]

decreasing the conversion values at the same time relative to neat VE resin. This may be probably due to behavior of MWCNTs like a heat sink towards the end of the reaction, as the temperature rises due to ongoing exothermic reaction in the system. In other words, CNTs influence the diffusion enhanced reaction during propagation stage dependent on functional groups attached to their surfaces.

Figures 10 and 11 show the Raman spectra of the CNTs used in this study and their corresponding nanocomposites, respectively. In principle of RS, it is required that area of peaks is compared on the same spectrum, not from one Raman spectrum to another. However, the intensity ratio of one peak to another can be used across the same Raman spectrum to monitor and identify chemical reactions involved.[15] In this manner, a regular peak that remains unchanged throughout the measurements is taken into account to trace the differences in the areas of the corresponding peaks. As depicted in Figure 10, Raman spectrum of CNTs is typically comprised of four different regions.[22] These are the graphite lattice vibrations, G band (1600 cm^{-1}), structural defects D band (1300 cm^{-1}) the G' band (2600 cm^{-1}) and the low frequency Radial Breathing Modes (RBMs), which corresponds to the collective radial movement of the carbon atoms. RBM is considered to get information regarding diameter and chirality's of the CNTs. Our main emphasis herein is on the G and D bands of the CNTs because they are hypothetically remained constant without being affected by the reaction that takes place in the system. In RS, C=C bonds for VE resin are visible at

1582 cm^{-1} (aromatic), 1604 cm^{-1} (aromatic), 1667 cm^{-1} (aliphatic). As stated earlier, these peaks are overlapped with the peaks of G and D bands. Note that the resin blend was used for RS measurements, but we followed the shifts in peaks of VE resin, as in the case of FTIR to ease the process of data interpretation. Following the procedure described earlier, the spectra obtained from the RS measurements were evaluated. As a result, it was found that CNTs with and without amine functional groups partially interrupted the C=C bonds of resins, which is principally proportional to the findings obtained from FTIR studies. In greater details, following the subtraction of the peaks from each other, the reduction in the peak areas relative to neat resin was observed to be 5% larger for nanocomposites with MWCNTs than those with MWCNT-NH$_2$. This is ample evidence that amine groups over the surfaces of CNTs changed the individual conversions of the monomers in the resin system, which is consistent with the findings obtained from FTIR studies.

Figure 12 depicts the typical thermal weight curvature achieved at constant heating rate of 5 °C/min for the cured neat polymer and its nanocomposites containing 0.3 wt % of MWCNTs and MWCNT-NH$_2$, respectively. Please note that the same trend was also confirmed using different heating rates (10 and 20 °C/min) in TGA experiments. Three experiments for each sample were performed. Although there was no significant difference in 5 wt % degradation temperatures (T_d)
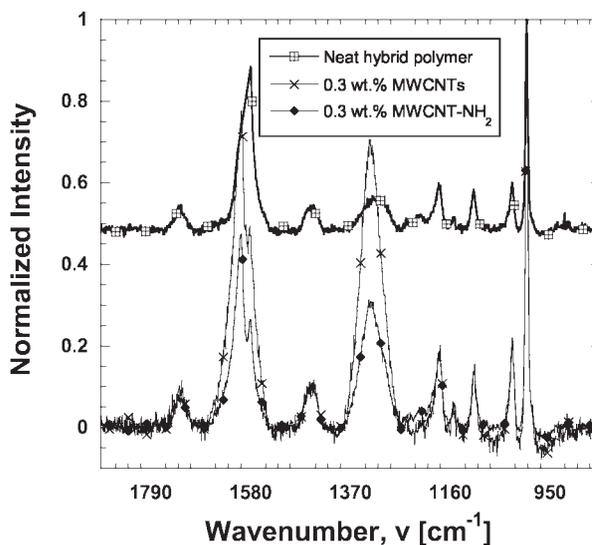
Figure 11. Raman spectra of the cured polymer and its corresponding nanocomposites with 0.3 wt % MWCNTs and MWCNT-NH$_2$.
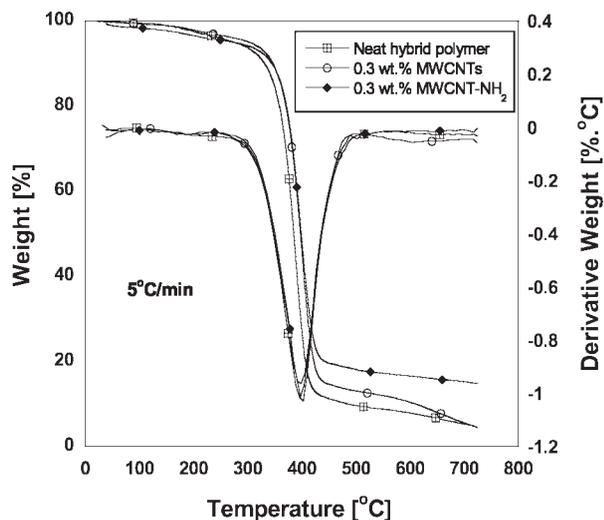
Figure 12. TGA thermograms of the cured neat resin and its corresponding nanocomposites containing 0.3 wt % of MWCNTs and MWCNT-NH$_2$ at a constant heating rate of 5 °C/min.

of the cured neat polymer and its nanocomposites with MWCNTs and MWCNT-NH$_2$, at each constant heating rate, the char yields at 700 °C was always higher for nanocomposites with MWCNT-NH$_2$ as compared to neat polymer and nanocomposites with MWCNTs. This implies that relatively high thermal stability was accomplished with incorporation of MWCNT-NH$_2$. This result shows consistency with the other findings obtained from DSC, FTIR, and RS studies. On the other hand, the first derivative (DTG) of the neat resin and its nanocomposites showed that just one peak occurs between 250 and 490 °C. This implies that degradation of the nanocomposite samples is one-stage process regardless of whether they contain MWCNTs or MWCNT-NH$_2$. From that point of view, we can conclude that CNTs restrict the entanglement and mobility of polymer chains, thus increasing the T_g and thermal stability of the polymers without disrupting the major steps of free-radical polymerization, significantly. Furthermore, thermal degradation activation energies of the cured polymer and its nanocomposites with MWCNTs and MWCNT-NH$_2$ were calculated at 5 wt % conversion level, following the procedure described earlier in the experimental part. As a result, degradation activation energies of neat polymer and its nanocomposites containing MWCNTs and MWCNT-NH$_2$ were predicted to be 62 ± 4, 65 ± 7 and 69 ± 6 kJ/mol, respectively. Thus, it can be concluded that MWCNT-NH$_2$ modified nanocomposites exhibit

somewhat higher thermal stability as compared to neat resin and those with MWCNTs.

On the basis of the findings obtained, it was found that presence of amino groups over the surfaces of CNTs induce a compromise. They enhance the dispersion of CNTs in the resin system while impeding partially the polymerization reaction by disrupting C=C bonds of resin matrix that are supposed to react with styrene. However, this complex phenomena results in synergy because relatively high glass transition temperature and mechanical properties were obtained from nanocomposites containing amino functionalized carbon nanotubes, for the same matrix resin system used in this study, as elucidated in our earlier study.[18]

CONCLUSIONS

A study was carried out on the cure kinetics of a VE/polyester based resin containing 0.3 wt % of MWCNTs and MWCNT-NH$_2$. In this respect, various experimental techniques including DSC, FTIR, RS, and TGA were systematically conducted to reveal the effects of CNTs on free radical polymerization. Nonisothermal DSC measurements at different constant heating rates revealed that the presence of CNTs within the resin system alters the polymerization reaction by increasing the heat of cure while decreasing the activation energies (E_a). It was emphasized that relatively low aspect ratio of amino functionalized nanotubes may play a crucial role in alteration of the interfacial chemical interactions during polymerization. Consequently, the suspension with MWCNT-NH$_2$ exhibits much heat of cure, besides lower activation energies as compared to neat resin blend and the suspension with MWCNTs. The predicted DSC curves via autocatalytic kinetic model were in good agreement with those experimentally obtained. Furthermore, FTIR studies aimed to elucidate the impact of CNTs on the development of the network in a polymer matrix that polymerizes via radicals was performed on neat VE resin and its suspensions with the same content of MWCNTs and MWCNT-NH$_2$ as the resin. As a result, the final conversion of styrene exceeded the final conversion of VE double bonds in the resin suspensions with MWCNT-NH$_2$, while final conversion of VE is higher than that of styrene in the resin suspensions with MWCNTs. RS studies performed on the cured polymer and its nanocomposites show consistency

with FTIR findings such that amine functional groups over the surfaces of CNTs altered the chemical reactions within the resin system. On the other hand, TGA measurements revealed that CNTs increased the thermal stability of the matrix resin such that E_d values of the nanocomposites prepared with MWCNTs and MWCNT-NH$_2$ are higher than that of the cured polymer. Moreover, at each constant heating rate, it was found that nanocomposites with MWCNT-NH$_2$ exhibited higher char yields when compared with neat resin and those prepared with MWCNTs. On behalf of the findings achieved, it was concluded that amine functional groups over the surfaces of CNTs altered relative individual fractional conversions of double bonds in the resin system.

REFERENCES AND NOTES

1. Gojny, F. H.; Wichmann M. H. G.; Köpke, U.; Fiedler, B.; Schulte, K. Compos Sci Technol 2004, 64, 2363–2371.
2. Xie, H.; Liu, B.; Juan, Z. J Polym Sci Part B: Pol Phys 2004, 42, 3701–3712.
3. Puglia, D.; Valentini, L.; Kenny, J. M. J Appl Polym Sci 2003, 88, 452–458.
4. Bae, J.; Jang, J.; Yoon, S. Macromol Chem Phys 2002, 15, 203–209.
5. Roşu, D.; Mititelu, A.; Caşcaval, C. N. Polym Test 2004, 23, 209–215.
6. Jannesari, A.; Ghaffarian, S. R.; Mohammadi, N.; Taromi, F. A., Molaei A. Thermochim Acta 2005, 425, 91–107.
7. Caba, K. L.; Guerrero, P.; Mondragon, I.; Kenny, J. M. Polym Int 1998, 451, 333–338.
8. Kessler, M. R.; White, S. R. J Appl Polym Sci Part A: Polym Chem 2002, 40, 2373–2383.
9. Roşu, D.; Caşcaval, C. N.; Mustata, F.; Ciobanu, C. Thermochim Acta 2002, 383, 119–127.
10. Yang, H.; Lee J. Polym Compos 2001, 22, 202–214.
11. Macan, J.; Ivankovic, H.; Ivankovic, M.; Mencer, H. J. Thermochim Acta 2004, 414, 219–225.
12. Rodrigues, J. M. E.; Pereira, M. R.; Souza, A. G.; Carvalho, M. L.; Neto, A. A. D.; Dantas, T.; Fonseca, J. L. C. Thermochim Acta 2005, 427, 31–36.
13. Sanchez, E. M. S; Zavaglia, C. A. C.; Felisberti, M. I. Polymer 2000, 41, 765–769
14. Malek, J. Thermochim Acta 2000, 355, 239–253.
15. Lu, M. G.; Shim M. J.; Kim S. W. Thermochim Acta 1998, 323, 37–42.
16. Kosar, V.; Gomzi, Z. Eur Polym J 2004, 40, 2793–2802.
17. Stevanovic, D.; Lowe, A.; Kalyanasundaram, S.; Jar, P. Y. B.; Alego, V. O. Polymer 2002, 43, 4503–4514.
18. Seyhan, A. T.; Gojny, F. H.; Tanoglu, M.; Schulte, K. Eur Polym J 2007, 40, 2793–2799.
19. Li, L.; Sun, X.; Lee, L. J Polym Eng Sci 1999, 39, 646–653.
20. Dua, S.; Mc Cullough, R. L.; Palmase, G. R. Polym Compos 1999, 20, 379–391.
21. Gryschuck, O.; Kocsis, J. K.; Thomann R.; Kanya, Z.; Kiricsi, I. Compos A 2006, 37, 1252–1259.
22. Fiedler, B., Gojny, F. H.; Wichmann, M. H. G; Nolte, M. C. M.; Schulte K. Compos Sci Technol 2005, 44, 2563–2578
23. Flynn, J. H.; Wall, L. A. Polym Lett 1966, 19, 323–328.